

## Self-Assembled MnN Superstructure

Xiangdong Liu,<sup>\*</sup> Bin Lu, Takushi Iimori, Kan Nakatsuji, and Fumio Komori<sup>†</sup>

*ISSP, University of Tokyo, Kashiwanoha 5-1-5, Kashiwashi, Chiba 277-8581, Japan*

(Received 3 November 2006; published 7 February 2007)

Self-assembled MnN nanoislands have been prepared on Cu(001) substrate. The nanoislands show a square shape and a well-defined size. They are regularly arrayed with a periodicity of  $(3.5 \pm 0.1)$  nanometer and form a two-dimensional square superstructure. The MnN island superstructure is stabilized by a short-range mechanism. A structural model has been proposed to explain the self-assembly and the high quality of the superstructure.

DOI: [10.1103/PhysRevLett.98.066103](https://doi.org/10.1103/PhysRevLett.98.066103)

PACS numbers: 68.65.-k, 61.30.Hn, 68.37.Ef

Self-assembled nanostructures have attracted tremendous interest recently [1–9]. Among them, the ones with regular spatial array, uniform and well-defined geometric and structural characters are especially desirable. Scientifically, such uniform nanostructure assembly allows us to probe into the quantum mechanical effects induced by quantum confinement [4,10–12] using a number of conventional techniques. Technologically, only when uniformly well-defined geometry and structure are achieved, self-assembled nanostructures can be applied to electronic [13] and optoelectronic [14] devices and high-density recording media [15]. However, it is still a difficult challenge to prepare such high-quality nanostructures. Here we describe the fabrication of self-assembled manganese nitride nanoislands on the Cu(001) substrate. The nanoislands show a square shape and well-defined size. They are regularly arrayed with a periodicity of  $(3.5 \pm 0.1)$  nanometer and form a two-dimensional square superstructure. Different from the conventional stress-domain dominated self-assembly, the shape, size, and periodicity of the MnN islands do not change with their coverage, indicating the self-assembling is driven by a short-range mechanism.

The self-assembled MnN nanoislands can be reproducibly prepared in three steps in ultrahigh vacuum (UHV) chambers. First,  $0.9 \pm 0.1$  monolayer [ML, 1 ML = 1 layer of Cu(001) substrate atoms] Mn is deposited on an atomically clean Cu(001) substrate at room temperature (RT) using a commercial electron-beam evaporator (Focus, EFM). Next, the deposited Mn film is exposed to atomic nitrogen at RT until saturated. The atomic nitrogen was produced by a homemade ion gun. During exposing the sample to nitrogen, a positive voltage identical to that of the ion gun anode was applied to the sample to remove the sputtering effect. Finally, the self-assembled nanoislands are formed as in Figs. 1(a)–1(c) after annealing the sample in UHV at 300 °C for 20 min and subsequently at 360 °C for 30 min. The deposition sequence of Mn and N has no effect on the final structure and quality of the superstructure. The preparation can alternatively start with exposing a clean Cu(001) substrate to atomic nitrogen until a diffuse  $c(2 \times 2)$  low-energy electron diffraction (LEED) pattern is observed. Subsequently,  $0.9 \pm 0.1$  monolayer Mn is de-

posited on the nitrogen covered Cu(001) substrate. After the sample is annealed with the same procedure as the above, exactly the same MnN superstructure is obtained. The prepared nanoislands are thermally stable at least upon being heated at 550 °C for 6 h.

As the scanning tunneling microscope (STM) images [Figs. 1(a)–1(c)] show, the islands have a regular square shape. The square-shaped islands themselves form a two-dimensional (2D) square superstructure with the islands' sides oriented along the  $\langle 10 \rangle$  direction of the square substrate surface lattice. The periodicity of superstructure is  $3.5 \pm 0.1$  nm, 14 times as large as the interplanar spacing of the Cu(001) substrate. The preferential step direction is  $\langle 10 \rangle$  direction. Crossing over a single step, the position of the islands shifts by a half of the superstructure period along the step direction [Fig. 1(b)].

Figure 1(c) shows a high-resolution STM image of the islands. The imaged surface atoms are arrayed in a square lattice with the same orientation as the Cu(001) substrate atoms. Each island contains approximately  $10 \times 10$  such atoms. The lattice constant is slightly larger than that of Cu substrate, but the difference is estimated to be smaller than 10%. The apparent height of the islands is measured to be 0.19 nm, close to a single-step height of the Cu(001) substrate; see Fig. 1(d). It is noticed the surface atoms in the “holes” among four islands show the same atomic orientation as the islands.

The uniformity of island size and the high degree of periodicity are confirmed by LEED, see Fig. 2. Superstructured  $(1 \times 1)$  LEED patterns have been observed over a wide energy range. The  $(1 \times 1)$  principal spots indicate a square lattice for the island surface atoms as is resolved by STM. A  $(14 \pm 1)$ -by- $(14 \pm 1)$  supercell is deduced from the superspots, again in agreement with the island periodicity determined by STM. Furthermore, it has been found that the intensity of the outer  $(11)$  superspots as indicated by the arrows in Fig. 2 increases with decreasing the Mn coverage within the Mn coverage range of  $0.5 \sim 1$  ML. Our STM examinations found that, with reducing the Mn amount, the island coverage proportionally decreases while keeping the size, shape, and periodicity of the islands the same as the full-covered sample. These

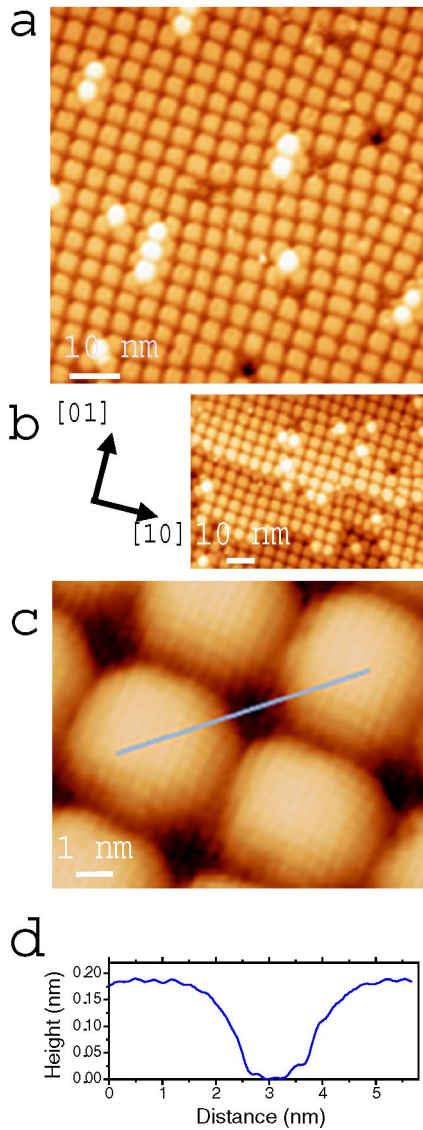


FIG. 1 (color online). (a) Large-scale STM image of the self-assembled MnN nanoislands on a wide terrace. The square-shaped islands form a two-dimensional square superstructure. (b) STM image showing that the island position shifts by a half superstructure constant at a single step along the step edge. (c) High-resolution STM image taken with a bias voltage of  $-2$  mV and a tunneling current of  $0.14$  nA. Cross section profile along the line is presented in (d). The orthogonality has been corrected for all the STM images in this Letter.

islands aggregate together leaving part of the Cu(001) surface clean [refer to Fig. 3(a)]. Using LEED and STM, we confirmed the presence of the clean Cu(001) surface by observing a  $c(2 \times 2)$  structure after we exposed the island partially covered sample to atomic nitrogen and subsequently annealed it at  $300^\circ\text{C}$  for 15 min in UHV[16]. Therefore, it is clear that the increased intensity of the outer (11) superspots is attributed to the increasing area of the clean Cu surface, which is superposed with the outer (11) superspots of the manganese nitride superstructure. There is no obvious intensification for the (01) outer super-

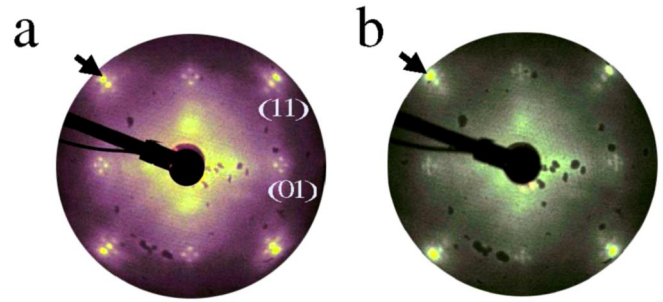


FIG. 2 (color online). LEED patterns of the island fully covered sample (a) and the partially covered sample (b) at  $114$  eV. The former contains  $(0.9 \pm 0.1)$  ML Mn, and the latter  $(0.75 \pm 0.08)$  ML Mn. The intensity of the outer (11) superspots as indicated by arrows increases upon decreasing the island coverage.

spots in Fig. 2, because the (01) diffraction intensity from clean Cu(001) at this electron energy ( $114$  eV) is very weak. At  $85$  eV, both the (01) and the (11) spots are bright in the LEED pattern of clean Cu(001). Then, we observed that all the outer superspots are intensified for partially covered samples. These observations allow us to confidently conclude that the lattice constant of the island surface atoms has expanded by  $(7.1 \pm 0.6)\%$  relative to the Cu(001) substrate.

The stoichiometry of the manganese nitride islands has been determined by *in situ* x-ray photoemission spectroscopy (XPS). We used a saturated Cu(001) $c(2 \times 2)$ -N surface as a reference sample for the calibration of the density of N atoms on the surface [16]. This surface contains exactly  $0.5$  ML N atoms. The integrated N  $1s$  XPS intensity from fully covered manganese nitride islands were reproducibly measured to be  $(1.8 \pm 0.2)$  times as large as that from Cu(001) $c(2 \times 2)$ -N. It is then determined that the formula of the manganese nitride is MnN.

This stoichiometry immediately remind us of the bulk MnN compound. Bulk MnN crystallizes into a face-centered tetragonal structure (distorted NaCl structure) with lattice constants of  $a = 4.256 \text{ \AA}$  and  $c = 4.189 \text{ \AA}$  [17]. The in-plane lattice constant of bulk MnN is larger than that of Cu(001) substrate by  $18.4\%$ . We propose that the present MnN islands adopt the same structure as its bulk correspondent. This is to say, the islands consist of a layer of Mn atoms and identical number of N atoms. Nitrogen atoms are located at the fourfold hollow position of the square Mn sublattice. However, different from bulk MnN, the 2D lattice of the MnN islands is only  $7.1\%$  larger than the substrate lattice. This structural model is consistent with the  $(1 \times 1)$  LEED pattern. It is reasonable that atomically resolved STM image shows a simple  $(1 \times 1)$  lattice, since STM does not always detect all the individual atoms but the local density of electronic states. Theoretically calculated STM images show the same situation for MgO monolayers on Ag(001) [18]. It is well known that the equilibrium in-plane lattice constant will decrease when the film thickness is reduced to monolayer range. For example, an  $8\%$  reduction in the in-plane lattice

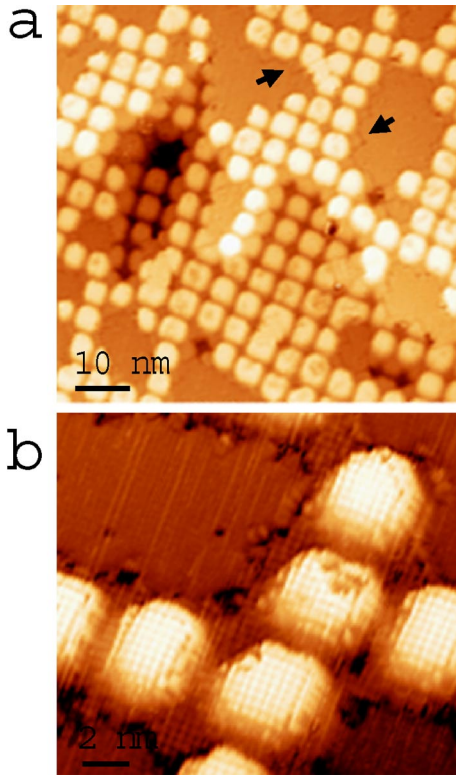


FIG. 3 (color online). (a) STM image of a sample partially covered by MnN islands. This sample contains 0.75 ML Mn. The MnN island superstructure has developed with the same island size and periodicity, leaving part of Cu(001) surface clean. (b) High-resolution STM image of isolated MnN island rows. Under this tip condition, the MnN surface is atomically resolved but the clean Cu(001) surface remains unresolved. The atomically resolved areas surrounding the MnN islands are MnN monolayer patches which are embedded in the substrate.

constant has been found for a 1 ML free-standing MgO slab [19]. Therefore, the actual mismatch between the MnN surface monolayer and the substrate should be less than 18.4%, but larger than 7.1% because of the interface-imposed stress. In addition, it should be pointed out that, we cannot exclude a tetragonal lattice distortion for the MnN islands which keeps the  $(1 \times 1)$  LEED pattern.

The self-assembling of the MnN islands cannot be explained using the conventional stress-domain mechanism. For most mismatched systems, the long-range repulsive elastic interaction between islands via the substrate is thought to be the essential factor for the self-organized growth [20]. In this case, a coverage-dependent separation between the neighboring islands [20–24] is normally expected. However, this is not the case for our MnN superstructure. As we mentioned above, the size, shape, and periodicity of the MnN islands are independent of the island coverage [see Fig. 3(a)]. This observation indicates that there should be a short-range mechanism to stabilize the superstructure. Moreover, the regular position shift of the MnN islands across the step is established both in the fully-covered and in the partially covered sample. This is

another feature distinguishing the present MnN superstructure from the self-organized islands governed by a stress-domain mechanism. In the latter case, because the stress field is deep into the subsurface [25], the perturbation of the stress field induced by a step is negligible so that the ordered structures on the lower terrace line up with those on the upper terrace [1,22].

We propose a new stress-relief model in Fig. 4 to explain the formation of the MnN superstructure. In this model, the whole surface is covered by a MnN monolayer, but the MnN monolayer splits into two layers. The top layer consists of the square islands as seen in Figs. 1(a)–1(c). The lattice of the MnN islands has expanded by 7.1%, as we observed by STM and LEED. The second layer is a single step lower than the top layer; i.e., it is embedded in the Cu(001) substrate. The embedded MnN monolayer covers the remaining areas of the surface and appear as the grid in Figs. 1(a)–1(c). Since the equilibrium lattice of MnN monolayer is larger than that of Cu(001), the square MnN islands tend to expand the underlying Cu(001) lattice. On the contrary, the MnN grid tends to compress the Cu lattice in the same layer. As a result of cancellation of these two effects, the Cu lattice is nearly unstrained. By the split growth, the free-energy of the whole system is minimized for the following reasons: (1) because of the long-range property, the elastic energy in the substrate is an important contribution to the gain in free-energy for a monolayer-thick misfit system; here this contribution has almost been removed. (2) Though the MnN grid is strained, its contribution to the gain of the free-energy is limited because of its small coverage; (3) the split growth allows the in-plane lattice of the MnN islands to be partially relaxed, which lowers the free-energy further. In this model, the width of the MnN grid and the size of the MnN islands are intrinsically defined by the stress equilibrium, i.e., the cancellation of the two stress imposed on the subsurface Cu lattice by the MnN islands and grid, respectively. Hence they are independent of the MnN island coverage. At the same time, the MnN superstructure is formed after being annealed at 360 °C and stable at higher temperature, so it is a thermodynamically equilibrium structure. The final structure is determined by the intrinsic energetics. This explains the structural perfection of the superstructure.

Other observations can also be explained within our model. For the isolated island rows on the samples partially covered by MnN islands, we have consistently observed that there always exist MnN patches in the terrace surrounding the MnN islands. These patches are a single step lower than the island and located in the same layer as the substrate topmost Cu atoms. A typical high-resolution STM image is shown in Fig. 3(b), where the MnN lattice is atomically resolved while the clean Cu(001) lattice remains unresolved. The embedded MnN patches accompanied with the MnN islands are also observed on the outskirts of compact MnN island assemblies as indicated by arrows in Fig. 3(a). These observations are in agreement

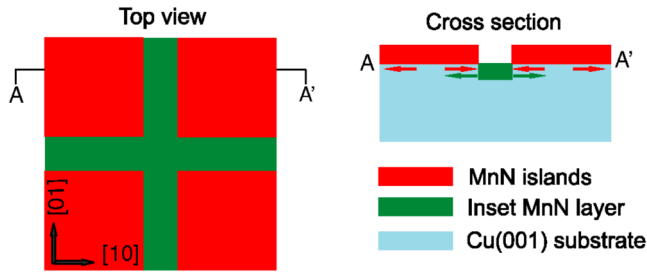


FIG. 4 (color online). Schematic model for the self-assembled MnN superstructure. The MnN monolayer covers the whole surface but splits into two layers. The top layer is seen as an array of the square islands whose lattice is relaxed and larger than that of the Cu(001) substrate. The second layer appears as the grid whose lattice is almost registered with the substrate. The stresses exerted on the topmost Cu layer underneath the MnN islands by the islands and the grid are illustrated by red and green arrows, respectively. See text for more explanations.

with our model that the simultaneous appearance of the MnN island with adjoining embedded MnN patches will reduce the stress in the substrate and thus is energetically favored.

The position shift of the islands across a step [see Fig. 1(b)] can be understood in our model. For the convenience of discussion, we refer to the positions of Mn and N perfectly registered with the substrate as normal positions. In our model, the embedded MnN grid is stressed and registered with the substrate. On the other hand, the lattice of MnN islands is expanded by 7.1% with respect to the substrate. In this case, only the atoms at the center of the island stay at their normal positions because of symmetry. The other atoms deviate from their normal positions more or less depending on their displacements from the island center. If only the component parallel to the step is considered, the deviation from their normal positions is minimum for the island atoms in a narrow strip zone which is perpendicular to the step and located in the middle of the island. Therefore, a shift of a half of the superstructure period allows this strip to be in line with the MnN grid so that the Mn and N atoms of the grid embedded in the upper terrace match those of the square islands on the lower terrace well without lattice distortion in the adjoining place. The above consideration does not exclude the case that the islands on the lower and upper terrace line up with each other without position shift. However, this case is energetically unfavorable, because the total step length will increase by 30–40%. As deduced from our model, a step contributes little to stress relaxation since the substrate Cu atoms are originally unstressed. Therefore an increase in step length leads to a net increase in the total free-energy of the system.

We notice that, most likely, our model can also apply to the saturated  $c(2 \times 2)$  N/Cu(001) system [26]. On this surface, narrow, single-step deep trenches which are also covered by  $c(2 \times 2)$  N are observed. On the basis of their careful STM observations, the authors of Ref. [26] con-

cluded that these trenches contribute little to the lateral stress relaxation of the  $c(2 \times 2)$  N overlayer, but are energetically favored in spite of the increased step energy. We think that the driving force of forming these trenches is a reduction of the N-overlayer induced strain in the underlying Cu layers. The trenches serve the same function as the MnN grid here in lowering the system's free-energy.

The authors thank D. Sekiba for his collaboration in the XPS measurement. One of the authors (X.L.) acknowledges support from JSPS.

\*Electronic address: liuxd@hust.edu.cn

Permanent address: School of Materials Science and Technology, Huazhong University of Science and Technology, Wuhan, 430074, People's Republic of China.

†Electronic address: komori@issp.u-tokyo.ac.jp

- [1] F. M. Leibsle, C. F. J. Flipse, and A. W. Robinson, *Phys. Rev. B* **47**, 15 865 (1993).
- [2] D. Leonard, M. Krishnamurthy, C. M. Reeves, S. P. Denbaars, and P. M. Petroff, *Appl. Phys. Lett.* **63**, 3203 (1993).
- [3] J. M. Moison *et al.*, *Appl. Phys. Lett.* **64**, 196 (1994).
- [4] R. Nötzel, J. Temmyo, and T. Tamamura, *Nature (London)* **369**, 131 (1994).
- [5] H. Brune, M. Giovannini, K. Bromann, and K. Kern, *Nature (London)* **394**, 451 (1998).
- [6] K. Pohl *et al.*, *Nature (London)* **397**, 238 (1999).
- [7] M. Corso *et al.*, *Science* **303**, 217 (2004).
- [8] J. V. Barth, G. Costantini, and K. Kern, *Nature (London)* **437**, 671 (2005).
- [9] K. Thürmer, R. Q. Hwang, and N. C. Bartelt, *Science* **311**, 1272 (2006).
- [10] M. F. Crommie, C. P. Lutz, and D. M. Eigler, *Science* **262**, 218 (1993).
- [11] Y. Guo *et al.*, *Science* **306**, 1915 (2004).
- [12] J. Y. Marzin, J. M. Gérard, A. Izraël, D. Barrier, and G. Bastard, *Phys. Rev. Lett.* **73**, 716 (1994).
- [13] B. Yu and M. Meyyappan, *Solid-State Electron.* **50**, 536 (2006).
- [14] A. P. Alivisatos, *Science* **271**, 933 (1996).
- [15] S. Sun, C. B. Murray, D. Weller, L. Folks, and A. Moser, *Science* **287**, 1989 (2000).
- [16] F. Komori, S. Ohno, and K. Nakatsuji, *J. Phys. Condens. Matter* **14**, 8177 (2002).
- [17] K. Suzuki *et al.*, *J. Alloys Compd.* **306**, 66 (2000).
- [18] N. Lopez and S. Valeri, *Phys. Rev. B* **70**, 125428 (2004).
- [19] L. Giordano, J. Goniakowski, and G. Pacchioni, *Phys. Rev. B* **67**, 045410 (2003).
- [20] V. A. Shchukin and D. Bimberg, *Rev. Mod. Phys.* **71**, 1125 (1999).
- [21] H. Ellmer *et al.*, *Surf. Sci.* **476**, 95 (2001).
- [22] K. Kern *et al.*, *Phys. Rev. Lett.* **67**, 855 (1991).
- [23] P. Zeppenfeld, M. Krzyzowski, C. Romainczyk, G. Comsa, and M. G. Lagally, *Phys. Rev. Lett.* **72**, 2737 (1994).
- [24] R. Plass, J. A. Last, N. C. Bartelt, and G. L. Kellogg, *Nature (London)* **412**, 875 (2001).
- [25] C. Cohen *et al.*, *Surf. Sci.* **490**, 336 (2001).
- [26] S. M. Driver and D. P. Woodruff, *Surf. Sci.* **492**, 11 (2001).